

# Evidence of thermal disequilibrium in contact binaries

H. Kähler

Hamburger Sternwarte, Gojenbergsweg 112, D-21029 Hamburg, Germany

Received 1 May 1996 / Accepted 3 July 1996

**Abstract.** We present a test which is sufficient to disprove thermal equilibrium in observed contact binaries. The test is applied to a number of systems with good spectroscopic data. All of them are shown to be in thermal imbalance. Accordingly, many (possibly all) contact binaries evolve on a thermal time-scale, probably in thermal cycles as proposed by Lucy (1976) and Flannery (1976).

**Key words:** stars – binaries – close

---

## 1. Introduction

In a preceding paper (Kähler 1995, hereafter K95) we investigated the conditions for thermal equilibrium in contact binaries. In unevolved (or slightly evolved) late-type systems the conditions are generally severe since rapid internal mass motions in the primary's envelope are required. We failed to notice that highly supersonic mass motions in the primary's outer layers are incompatible with the observed broadening of spectral lines. Combining this observational fact with the results of K95 we already have a strong argument that unevolved or slightly evolved systems are usually in thermal disequilibrium, in accordance with the results of Lucy (1976), Flannery (1976) and Robertson & Eggleton (1977).

For evolved systems, however, the situation is less clear. Lucy (1976) suggested that A-type systems are evolved and in thermal equilibrium. Robertson & Eggleton (1977) and Refsdal & Stabell (1981) showed indeed the existence of evolved theoretical configurations in stable thermal equilibrium, but these configurations are possibly not realistic.

The purpose of the present paper is to show that thermal equilibrium in late-type contact binaries, evolved or not, usually cannot be established. Sect. 2 concerns theoretical contact configurations in thermal equilibrium. In Sect. 3 we discuss observational properties of contact binaries and derive a test which is (within the framework of some assumptions) sufficient to disprove thermal equilibrium in an observed system. This test is applied to a number of W-type and A-type systems. Sect. 4 concerns uncertainties in the present analysis. In the last section the results are summarized.

## 2. Theoretical equilibrium configurations

Approximate structure equations for contact systems in thermal equilibrium have been derived in K95, allowing for the effects of large-scale mass motions in the common turbulent envelope.

### 2.1. The surface condition

On account of these mass motions the Roche equipotential condition is replaced by a more general surface condition. The underlying assumptions require some comments.

Neglecting turbulent viscosity in the Navier-Stokes equations for steady motions we obtained Bernoulli's equation for a stream line  $\sigma$  on the surface

$$\Psi_R + \frac{v^2}{2} = \text{constant} \quad \text{on } \sigma, \quad (1)$$

where  $\Psi_R$  denotes the Roche potential and  $v$  is the velocity of the mass motions in a rotating frame.

If all streamlines meet in stagnation points, as in the velocity field proposed by Webbink (1977), the constant is the same for all streamlines and we find

$$\Psi_R + \frac{v^2}{2} = \text{constant} \quad \text{on } \Sigma, \quad (2)$$

where  $\Sigma$  denotes the surface. This equation gives a generalised surface condition (Eq. 20 in K95). The presence of internal mass motions is expressed by parameters  $\eta_1$  and  $\eta_2$  representing respectively the average of the squared velocity on the surface of the component 1 and 2. They are defined by

$$\langle v^2 \rangle = \frac{2}{3} \omega^2 R_i^2 \eta_i, \quad (3)$$

where  $\omega = 2\pi/P$  with  $P$  = period is the angular velocity of the system,  $R_i$  is the radius of the component  $i$  and the angle brackets denote a spherical average.

In the general case there are closed streamlines on the surfaces of both components and the area  $\Sigma$  in Eq. (2) must be replaced by  $\Sigma/\Delta$ , where  $\Delta$  is the region enclosed by these streamlines. The generalised surface condition remains an approximation with a modified interpretation of  $\eta_i$ . This parameter represents the average of the squared velocity on a part of the surface of the component  $i$  (at least a belt around the equator).

If  $\eta_1$  and  $\eta_2$  are small compared to unity, the departures from Roche geometry are small. In the absence of internal mass motions ( $\eta_1 = \eta_2 = 0$ ) the generalised surface condition reduces to the Roche equipotential condition.

## 2.2. Hydrostatic equilibrium

As shown in K95, internal mass motions in the envelope  $i$  can approximately be characterized by two parameters  $\omega_i$ ,  $c_i$ , where  $\omega_i$  expresses the mean kinetic energy of these motions and the coefficient  $c_i$  expresses the correlation of these motions with the orbital motion. The motions are rapid (comparable with the orbital velocity) if  $\omega_i/\omega$  is of order unity, and slow compared with the orbital velocity if

$$\omega_i \ll \omega. \quad (4)$$

If this inequality is satisfied, the effects of internal mass motions are small. The effects on the surface condition are of the second order in  $\omega_i/\omega$  since  $\eta_i = (\omega_i/\omega)^2$ .

The spectral line broadening of typical contact binaries is consistent with the assumption that the internal mass motions are slow compared with the orbital velocity (cf. Ruciński et al. 1993 and references therein). Rapid motions are almost certainly incompatible with the observed broadening functions. For this reason the inequality (4) will be treated as an observational constraint.

Using this constraint we conclude that the effects of internal mass motions are very small. In other words, thermal equilibrium implies approximate hydrostatic equilibrium. In the further discussion hydrostatic equilibrium will be assumed.

## 2.3. The degrees of freedom

We shall consider configurations in good thermal contact. Accordingly, we assume that the equal entropy condition

$$\Delta S := S_1 - S_2 = 0 \quad (5)$$

is satisfied, where  $S_k$  denotes the specific entropy in the adiabatic part (more precisely, at the inner border) of the convective envelope  $k$ . The mixing-length in units of the pressure scale height will be taken to be  $\alpha = 1.5$ .

Let  $\Psi$  denote the Roche potential on the surface, and  $\Psi_j$  the potential in the Lagrangian point  $L_j$ . The degree of contact  $F$  is defined by

$$F = (\Psi - \Psi_1)/(\Psi_2 - \Psi_1), \quad (6)$$

and the contact condition is

$$0 < F \leq 1. \quad (7)$$

When discussing the degrees of freedom we include also unphysical configurations violating the contact condition.

The physical parameters of a stationary system are mass  $M$ , total angular momentum (the sum of orbital and spin angular momentum)  $J$  and composition. Concerning the composition,

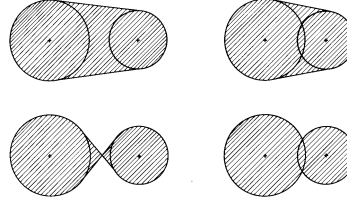


**Fig. 1.** Two approximations for the projected area of a contact binary. The area is either overestimated (top) or underestimated (bottom)

for the hydrogen content in the envelope a standard value  $X = 0.7$  will be adopted. Evolutionary effects in the primary can roughly be taken into account adopting the simple hydrogen profile

$$X = \begin{cases} X_c + (0.7 - X_c) \sin\left(\frac{\pi}{2} \frac{\xi}{\xi_c}\right) & \text{if } \xi < \xi_c \\ 0.7 & \text{otherwise,} \end{cases} \quad (8)$$

where  $\xi = m_1/M_1$  and  $m_1$  is the mass variable. Evolutionary effects in the secondary are much smaller and will be neglected. The composition is then described by the metallicity  $Z$ , the hydrogen content in the primary's centre  $X_c$  and the fractional extent of the primary's evolved core  $\xi_c$ . Unless stated otherwise,  $\xi_c = 0.5$  will be assumed.

With these approximations we have the four physical parameters  $M, Z, X_c, J$ . Basic observational data are period  $P$  and mass ratio  $q$ . The angular momentum can be replaced by one of these quantities. Accordingly, if four of the five parameters  $M, Z, X_c, P, q$  are given, the configuration is usually (at least locally) determined uniquely.

## 2.4. Thermal stability

The thermal stability problem concerns perturbations in the distribution of entropy. The perturbed system is supposed to be in hydrostatic equilibrium and uniform rotation and to satisfy the equal entropy condition. Mass and total angular momentum and the composition of each mass element are kept fixed. With these definitions the thermal stability problem is uniquely defined. Note that (on account of perturbations in the mass ratio) the chemical profile of a perturbed system is not described by Eq. (8). The stability can be tested either in a stability analysis (i.e. in a discussion of the eigenvalues of the stability problem) or studying the evolution, starting with a small perturbation.

This stability problem is formally applicable also to systems violating the contact condition. (Physically, equal entropy requires contact, but this point is unimportant in a formal stability discussion.) Other thermal stability problems can be obtained on replacing the equal entropy condition by another equation. The connection between different thermal stability problems will be discussed in Sect. 4.

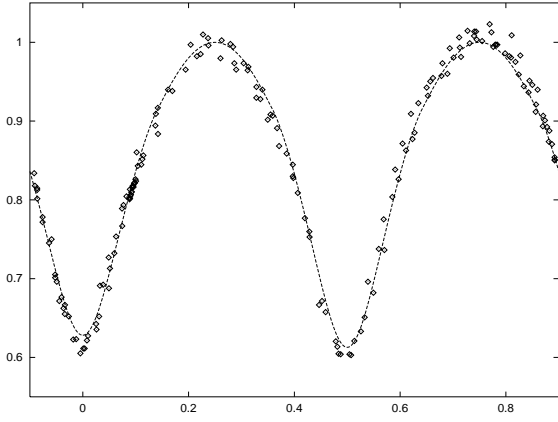


**Fig. 2.** Observed and theoretical light curves of BV Dra (see text)

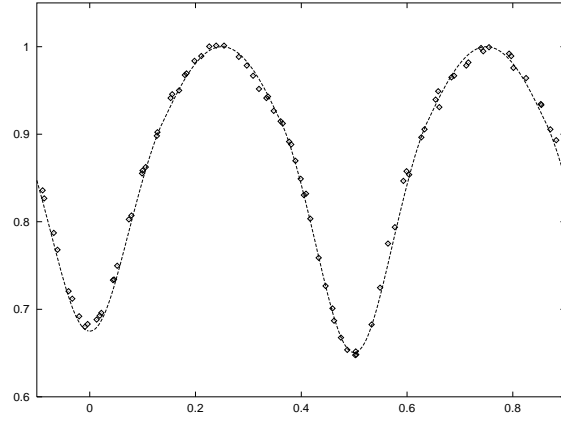


**Fig. 3.** Observed and theoretical light curves of BW Dra (see text)

### 2.5. Theoretical light curves

For comparison with the observations we shall need theoretical light curves. Here we present a simple light curve synthesis without reference to Roche geometry.

Input parameters are the spherically averaged radii  $R_1, R_2$  and the effective temperatures  $T_{e1}, T_{e2}$  of the components, their separation  $A$  as obtained by Keplers law

$$\omega^2 = GM/A^3 \quad (9)$$

and the inclination angle  $i$ . Normalized radii  $\lambda_1, \lambda_2$  of the components and the ratio of temperatures  $\tau$  are defined by  $\lambda_i = R_i/A$ ,  $\tau = T_{e2}/T_{e1}$ . The separation  $A$  will be taken as the unit of length. Let  $s$  be the projected separation and  $B$  the projected area of the system. The components will be treated as spheres of radii  $\lambda_1, \lambda_2$ , apart from the neck near the inner Lagrangian point. Two approximations for the neck are shown in Fig. 1. In the first approximation the projected area is overestimated, i.e. we obtain an area  $B_{\max} > B$ . In the second approximation the area is underestimated ( $B_{\min} < B$ ). We shall take the average

$$B = (B_{\max} + B_{\min})/2. \quad (10)$$

Next we make use of the approximations to split the area  $B$  into the contributions of the components, writing  $B = B_1 + B_2$ . The distribution of surface brightness is then approximately determined by the parameter  $\tau$ .

It remains to give explicit expressions for these areas. In the case of  $s \leq \lambda_1 - \lambda_2$  we have either an occultation with

$$B_1 = \pi\lambda_1^2, \quad B_2 = 0 \quad (11)$$

or a transit with

$$B_1 = \pi(\lambda_1^2 - \lambda_2^2), \quad B_2 = \pi\lambda_2^2. \quad (12)$$

In the case of  $s \geq \lambda_1 - \lambda_2$  we obtain

$$B_{\max} = s(\lambda_1 + \lambda_2) \cos \vartheta + \left(\frac{\pi}{2} + \vartheta\right)\lambda_1^2 + \left(\frac{\pi}{2} - \vartheta\right)\lambda_2^2 \quad (13)$$

with  $\vartheta = \arcsin((\lambda_1 - \lambda_2)/s)$ . In the subcase of  $s \geq \lambda_1 + \lambda_2$  we find

$$B_{\min} = (\lambda_1^2 + \lambda_2^2) \left( \frac{s \cos \vartheta}{\lambda_1 + \lambda_2} + \frac{\pi}{2} + \xi \right) \quad (14)$$

with  $\xi = \arcsin((\lambda_1 + \lambda_2)/s)$ , and finally

$$B_i = \frac{\lambda_i^2}{\lambda_1^2 + \lambda_2^2} B \quad (i = 1, 2). \quad (15)$$

In the remaining subcase of  $s < \lambda_1 + \lambda_2$  we have

$$B_{\min} = \sum_{i=1}^2 \lambda_i^2 \left( \pi + \frac{\beta_i - \sin \beta_i}{2} \right) \quad (16)$$

with

$$\beta_i = 2 \arccos \frac{s^2 + (-1)^i (\lambda_2^2 - \lambda_1^2)}{2s\lambda_i}. \quad (17)$$

If the primary is in front of the secondary, the final result is

$$B_1 = \frac{\pi\lambda_1^2}{B_{\min}} B, \quad B_2 = B - B_1. \quad (18)$$

If the secondary is in front of the primary, the indices 1 and 2 must be interchanged.

The systems BV Dra and BW Dra can be used to test this simple light curve synthesis. Light curves of BV Dra (Yamasaki 1979) and BW Dra (Ruciński & Kaluzny 1982) and spectroscopic observations of both systems (Batten & Lu 1985) were used by Kaluzny & Ruciński (1986, hereafter KR86) to derive the following parameters:

$$\begin{aligned} \text{BV Dra: } & i = 76.28, \quad \lambda_1 = 0.472, \quad \lambda_2 = 0.318, \quad \tau = 1.016, \\ \text{BW Dra: } & i = 74.42, \quad \lambda_1 = 0.499, \quad \lambda_2 = 0.281, \quad \tau = 1.031. \end{aligned}$$

Theoretical light curves with these parameters as obtained by the present simple procedure are shown in Figs. 2 and 3, together with the observed light curves. The agreement is rather good for BV Dra (the theoretical light curve is somewhat too shallow) and very good for BW Dra. A comparison with the theoretical light curves of KR86 shows that the present results are only slightly inferior. Accordingly, effects neglected in the present light curve synthesis are of minor importance.

### 3. Thermal imbalance of observed contact binaries

#### 3.1. Observational properties

From the observational data a few global parameters can be determined. The period is exactly known. The mass ratio and a lower limit  $M \sin^3 i$  for the total mass can be found from radial velocities. The temperature difference  $\Delta T_e = T_{e1} - T_{e2}$  and the mean effective temperature  $T_e$  can be approximately determined from the colours and spectral types of the components.

If the spectroscopic mass ratio is known, additional properties (e.g. mass  $M$ , light ratio  $L_2/L_1$ , degree of contact  $F$ ) can be determined in a light curve analysis, but the results are often uncertain. For this reason the light curve will be used directly (i.e. without interpretation in a light curve analysis) as an observational property.

#### 3.2. The temperature difference

In many observed systems the secondary is hotter than the primary. In theoretical configurations with typical mass ratios however the primary is slightly hotter than the secondary, i.e.  $\Delta T_e$  is positive. For systems in good thermal contact this follows from the equal entropy condition (5) and Lucy's (1967) discussion (in hydrostatic equilibrium the mean effective gravity is slightly larger in the primary than in the secondary). If the thermal contact is poor, the entropy difference  $\Delta S$  is positive and the temperature difference is even larger.

If these theoretical results are reliable, observed systems with a negative temperature difference are far from hydrostatic equilibrium and thus not in thermal equilibrium.

The theoretical temperature difference is however only an approximation. A mixing-length formalism is used to calculate the temperature gradient, and the mixing-length  $\alpha$  is assumed to be the same in both components. On account of these approximations the argument against thermal equilibrium is not conclusive.

Summarizing, a negative observed temperature difference (and the resulting properties of the light curve) cannot be explained in the present theoretical treatment since in hydrostatic equilibrium the theoretical difference is always positive. Both differences are however small and can be neglected in an approximate discussion.

#### 3.3. Test of thermal imbalance

Consider an observed system with reliable spectroscopic values for  $q$  and  $M \sin^3 i$ . We shall ask whether the system can be in thermal equilibrium.

For this purpose we have to check all theoretical equilibrium configurations with the given (observed) values of period and mass ratio. As shown in Sect. 2.3 they can be approximately described by two parameters. For some choice of these parameters, the properties of the theoretical configuration must be compatible with the observations, the contact condition (7) must be satisfied, and the configuration must be thermally stable. Other-

wise thermal equilibrium can be excluded within the framework of our approximations.

Taking into account the observable properties as collected in the preceding subsections, the result can be summarized as follows. If an observed system is in thermal equilibrium, there exists a theoretical equilibrium configuration with the observed values of period and mass ratio having the following properties: (I) The mean effective temperature  $T_e$  is compatible with the observations. (II) The theoretical light curve is compatible with the observed light curve, with the possible exception of differences between the two minima. Note that the inclination of a theoretical configuration is known from the mass  $M$  and the observed value of  $M \sin^3 i$ . The theoretical light curve is therefore also known. (III) The contact condition (7) is satisfied. (IV) The configuration is thermally stable.

For given period and mass ratio, a theoretical equilibrium configuration has two degrees of freedom. They can usually be adjusted to satisfy the conditions (I) and (II). (An exception concerns systems with a very high inclination. Since the mass is approximately known from the observed value of  $M \sin^3 i$ , there is no freedom to satisfy two conditions.) The resulting configuration is determined uniquely if uncertainties in the observational input parameters and the theoretical treatment are ignored. If these uncertainties are taken into account we obtain a set of theoretical configurations with the properties (I) and (II). If any one of these configurations satisfies the conditions (III) and (IV), nothing more can be said. The observed system may or may not be in thermal equilibrium. (The conditions for thermal equilibrium are necessary but by no means sufficient.) However, if configurations satisfying the contact condition do not exist, or if all of them are thermally unstable, the observed system is certain to be in thermal imbalance.

In the following subsections this test will be applied to a number of observed systems. We begin with a detailed discussion of the system BV Dra. For the other systems a short discussion will be sufficient.

#### 3.4. Thermal imbalance of BV Dra

For the system BV Dra (period  $P = 0.35007$  day) Batten & Lu (1985) determined the parameters  $q = 0.402$ ,  $M \sin^3 i = 1.277 M_\odot$  and found that the secondary (spectral typ F8) is slightly hotter than the primary (F9). KR86 determined from the colours a mean effective temperature  $T_e = 6190$  K. Strömgen colours (Ruciński 1983) and the calibration of Philip & Relyea (1979) give  $T_e \simeq 6000$  K. To cover this range we investigated models with temperatures of 6000, 6100 and 6190 K.

Properties of configurations satisfying the conditions (I) and (II) are listed in Table 1. The contact condition (III) is also satisfied. The theoretical light curves have been fitted to the observed light curve during the transit eclipse, cf. Fig. 4. The temperature difference is positive and too large. This implies that during the occultation eclipse the theoretical light curve is too shallow. Except for these difficulties (which are unavoidable as discussed in Sect. 3.2) the observed properties of BV Dra are reproduced.

**Table 1.** Theoretical configurations in thermal equilibrium for comparison with BV Dra

$M/M_{\odot}$	$Z$	$X_c$	$T_e$	$\Delta T_e$	$F$	$L/L_{\odot}$
1.37	.00826	.1586	6000	72	.733	2.36
1.37	.00708	.1587	6100	70	.724	2.51
1.37	.00603	.1575	6190	68	.720	2.66

Condition (IV) however is violated. The configurations are thermally unstable with an  $e$ -folding time of about  $4 \cdot 10^7$  yr. This was shown in an eigenvalue analysis as well as in evolutionary calculations. Accordingly, within the framework of our approximations (this caveat will be made also in the following subsections) BV Dra is certain to be in thermal imbalance.

### 3.5. Thermal imbalance of BW Dra

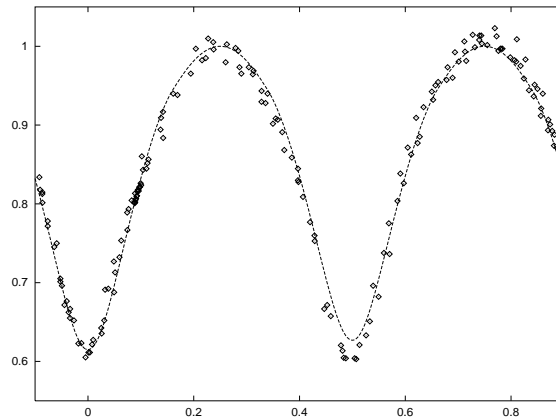
For the system BW Dra ( $P = 0.29217$  day) Batten & Lu (1985) determined the parameters  $q = 0.280$ ,  $M \sin^3 i = 1.013 M_{\odot}$ . Strömgen colours (Ruciński 1983) and the calibration of Olsen (1984) give a mean effective temperature  $T_e = 5664$  K. For the primary KR86 derived an effective temperature of about 5900 K. For temperatures in this range, conditions (I) and (II) give evolved ( $X_c \simeq 0.19$ ) configurations of mass  $M \simeq 1.2 M_{\odot}$ . Since the contact condition is violated ( $F \simeq 1.3$ ), thermal equilibrium can be excluded. In the generalised (formal) thermal stability problem the models are unstable on a time scale of about  $7 \cdot 10^7$  yr.

### 3.6. Thermal imbalance of W UMa

For the system W UMa ( $P = 0.33364$  day) Ruciński et al. (1993) determined from 1989 data the parameters  $q = 0.479$ ,  $M \sin^3 i = 1.747 M_{\odot}$ , a mean temperature of  $(6000 \pm 150)$  K and the mass  $M = 1.760 M_{\odot}$ . The light curve (e.g. Linnell 1991) shows that the inclination is very high. Accordingly, there is little freedom in the mass. Using these values of  $P, q, M$  and adopting the metallicity  $Z = 0.01$  we obtain an evolved ( $X_c = 0.367$ ) configuration with a mean temperature of 6370 K. The contact condition is violated ( $F \simeq 1.1$ ). For larger values of  $Z$  the temperature is lower but  $F$  is still larger. For these reasons thermal equilibrium can be excluded. The configurations are unstable on a time scale of about  $3 \cdot 10^7$  yr.

### 3.7. Thermal imbalance of AH Vir

The system AH Vir ( $P = 0.40753$  day) has also a very high inclination. Lu & Ruciński (1993) determined the parameters  $q = 0.303$ ,  $M \sin^3 i = 1.768 M_{\odot}$ , a mean temperature of 5300 K and a mass of  $1.77 M_{\odot}$ . Adopting this mass and the metallicity  $Z = 0.017$  we obtain an evolved ( $X_c = 0.386$ ) configuration which is much too hot ( $T_e = 6209$  K) and in severe conflict with the contact condition ( $F \simeq 1.3$ ). If the metallicity is increased,

**Fig. 4.** The light curve of the last model in Table 1 in comparison with the observed light curve of BV Dra

the temperature decreases but the conflict with the contact condition increases. Accordingly, AH Vir is in thermal imbalance. The configurations are unstable on a time scale of about  $5 \cdot 10^7$  yr.

### 3.8. Thermal imbalance of AB And

For the system AB And ( $P = 0.33189$  day) Hrivnak (1988) determined the parameters  $q = 0.491$ ,  $M \sin^3 i = 1.493 M_{\odot}$ . In a light curve analysis he found  $i = 86.8$ ,  $\lambda_1 = 0.451$ ,  $\lambda_2 = 0.327$ ,  $\tau = 1.068$ . Using these parameters, the present light curve synthesis is not able to reproduce the observed light curve. In the theoretical light curve the difference between the two minima is too large on account of the temperature difference.

The observed light curve shows that the inclination is very high. We calculated models of mass  $M = 1.5 M_{\odot}$  and mean temperatures between 5450 K (the primary's temperature adopted by Hrivnak) and 5800 K. The theoretical light curve is always too shallow. The models are evolved ( $X_c \approx 0.2$ ) and satisfy the contact condition ( $F = 0.8 \dots 0.9$ ). All of them are thermally unstable with an  $e$ -folding time of  $(5 \dots 7) \cdot 10^7$  yr. Accordingly, AB And is in thermal im

### 3.9. Thermal imbalance of V508 Oph

So far we discussed W-type systems. The A-type system V508 Oph ( $P = 0.344792$ ) has parameters similar to those of AB And and also a very high inclination. Lu (1986) and Lapasset & Gómez (1990) found  $q = 0.52$ ,  $M \sin^3 i = 1.52 M_{\odot}$  and determined a mean temperature between 5800 and 6000 K. We calculated models with these parameters and the mass  $M = 1.52 M_{\odot}$ . They are evolved ( $X_c \approx 0.2$ ) and satisfy the contact condition ( $F \approx 0.6$ ). The theoretical light curves are too shallow. All models are unstable on a time scale of  $(3 \dots 4) \cdot 10^7$  yr. We conclude that V508 Oph is in thermal imbalance.

**Table 2.** Effects of changes in the hydrogen content, the entropy difference, the mixing-length and the chemical profile (see text)

$X$	$\Delta S$	$\alpha$	$\xi_c$	$Z$	$X_c$	$\Delta T_e$	$F$	$\tau$
.7	0	1.5	.5	.0060	.1575	68	.720	3.72
.73	0	1.5	.5	.0043	.1402	64	.691	3.67
.7	0	1	.5	.0038	.1977	84	.919	2.79
.7	0	1.5	.4	.0057	.0594	65	.688	3.48
.7	.1	1.5	.5	.0060	.1607	82	.708	3.62
.7	.2	1.5	.5	.0060	.1639	96	.696	3.62

### 3.10. Thermal imbalance of OO Aql

The A-type system OO Aql ( $P = 0.50679$  day) has one of the largest mass ratios. Hrivnak (1989) determined the parameters  $q = 0.843$ ,  $M \sin^3 i = 1.918 M_\odot$  and a temperature between 5500 and 6000 K. The light curve indicates that the inclination is very high. We investigated models in hydrostatic equilibrium with  $M = 1.918 M_\odot$ . Adopting the metallicity  $Z = 0.035$  we obtain an evolved ( $X_c = 0.168$ ) model in severe conflict with the contact condition ( $F = -0.48$ ) and with a mean temperature of 4390 K which is much too low. Decreasing  $Z$  we obtain models with higher temperature but even lower degree of contact. Thermal equilibrium can therefore be excluded. The configurations are unstable on a time scale of about  $5 \cdot 10^7$  yr.

## 4. Discussion

In the preceding section we investigated a number of observed contact binaries. All of them turned out to be in thermal disequilibrium. The discussion was based on approximations. Are the results certain, i.e. unaffected by uncertainties in the discussion?

### 4.1. Arguments against thermal equilibrium

Essentially two arguments against thermal equilibrium have been used. The first argument concerns the structure of theoretical equilibrium configurations with given (observed) properties. Thermal equilibrium can be excluded when in conflict with the contact condition.

If this argument does not apply, i.e. if the contact condition can be satisfied (as in the case of BV Dra, AB And and V508 Oph), we need the second argument which concerns the stability of theoretical configurations with the given properties. Thermal equilibrium can be excluded when unstable. The stability properties depend not only on the structure of the configuration but also on assumptions on thermal perturbations.

### 4.2. Uncertainties in the structure

Here we ask for the effects of uncertainties in the structure of theoretical equilibrium configurations. We adopted the hydrogen content  $X = 0.7$ . In reality  $X$  may be somewhat larger. As an approximation we used the equal entropy assumption (5). In

**Table 3.** The  $e$ -folding time  $\tau$  (in units of  $10^7$  yr) of unstable configurations for fixed physical parameters and different values of  $\Delta S$ ,  $m$  and  $n$  (see text)

		$\Delta S$		
$m$	$n$	0.01	0.1	0.2
4.5	2	3.74	4.17	4.84
1	2	3.71	3.75	3.82
0	2	3.70	3.64	3.60
3	1	3.76	4.38	5.41
1	1	3.72	3.87	4.09

reality the entropy difference  $\Delta S$  is small but positive. A third uncertainty concerns the mixing-length  $\alpha$ .

Potentially most important is the uncertainty in the chemical profile. We used the approximation (8) with  $\xi_c = 0.5$ . In realistic profiles (e.g. Kippenhahn & Weigert 1990) the evolutionary effects are somewhat more concentrated to the centre. This corresponds to a smaller value of  $\xi_c$ .

Among all theoretical configurations investigated, evolutionary effects are most important ( $X_c$  is smallest) in the last model in Table 1. We compared this model with other models for the given observed properties (including a temperature of 6190 K). They are defined by the values for  $X$ ,  $\Delta S$ ,  $\alpha$  and  $\xi_c$ . The entropy difference is expressed as entropy per nucleus divided by Boltzmann's constant, and assumed to be constant in the course of a thermal perturbation.

Results are listed in Table 2. All models have the mass  $M = 1.37 M_\odot$ . The symbol  $\tau$  denotes the  $e$ -folding time of the most unstable mode in units of  $10^7$  yr. As expected, a decrease in  $\xi_c$  is compensated by a decrease in  $X_c$ . The results show that uncertainties in  $X$ ,  $\xi_c$  and  $\Delta S$  are unimportant for the properties of interest (degree of contact and instability). Uncertainties in the mixing-length have some influence, but the qualitative results are not affected. (It should be noted that the model with  $\alpha = 1$  is slightly inconsistent. The secondary's convective envelope is very shallow, and in the inner part of this envelope departures from adiabaticity are neglected.)

Uncertainties in the opacity have not been discussed. We used Los Alamos opacities.

### 4.3. Uncertainties in the stability problem

We adopted the equal entropy condition (5). If this condition is replaced by another equation, the stability properties may change. For example, we may assume that the entropy difference  $\Delta S$  is non-zero and constant. This is of little influence as shown in the preceding subsection. Alternatively, in a configuration satisfying the contact condition and having a positive entropy difference Eq. (5) can be replaced by the equation

$$\Lambda = KF^m(\Delta S)^n, \quad (19)$$

where  $\Lambda$  denotes the luminosity (in solar units) transferred from the primary to the secondary and  $K, m, n$  are constants. An equivalent equation was proposed by Hazlehurst & Refsdal (1980). If this equation is adopted, the stability properties depend on the structure (including  $\Lambda, F, \Delta S$ ) as well as on the coefficients  $m$  and  $n$ .

Are these uncertainties in the stability problem important? Since we are discussing systems in good thermal contact with deep convective envelopes, the entropy difference is small compared to unity. Since the mass ratios are far from unity,  $\Lambda$  is of order unity. Accordingly, if Eq. (19) is adopted,  $n$  must be taken to be positive and  $K$  must be sufficiently large. Under these circumstances small changes in  $\Delta S$  are sufficient for the adjustment of  $\Lambda$ , and the stability problem should (approximately) be independent of a stability problem based on the equal entropy assumption. In other words, uncertainties in the definition of the stability problem should be unimportant as long as the entropy difference is bound to be sufficiently small.

To check these arguments we investigated the effects of changes in the stability problem for given observed properties, taken again from the system BV Dra with a temperature of 6190 K. Adopting Eq. (19) we calculated the time scale  $\tau$  for different values of  $\Delta S, m$  and  $n$ . Reasonable values for  $m$  and  $n$  are uncertain, but the case of  $n \ll 1$  is certainly unrealistic since the adjustment of entropy between the components is inhibited. Hazlehurst & Refsdal (1980) presented arguments for  $m \geq 3, n \geq 1$  with a preference for  $m = 4.5, n = 2$ .

Results are listed in Table 3. For  $\Delta S = 0.01$  the time scale is almost independent of  $m$  and  $n$ , in accordance with the above arguments. If the entropy difference is larger  $\tau$  depends on  $m$  and  $n$ . An increase in  $m$  and a decrease in  $n$  have a stabilizing influence. For given positive values of  $m$  and  $n$ , an increase in  $\Delta S$  has also a stabilizing effect. The uncertainty in  $\tau$  is however not large.

This check was applied also to other observed systems, with similar results. Accordingly, uncertainties in the stability analysis are of minor importance since the instability is not affected.

## 5. Concluding remarks

We investigated a number of observed contact binaries in a broad range of periods and mass ratios. Each system was treated individually. Combining observed properties and an approximate treatment of theoretical configurations in thermal equilibrium we derived two arguments against thermal equilibrium. Thermal equilibrium can be excluded (1) when in conflict with the contact condition and (2) when unstable. In each system one of these arguments applies and thermal equilibrium can safely be excluded, provided that Los Alamos opacities are adequate.

We did not discuss systems with extremely small mass ratios such as TV Mus, XY Boo, AW UMa. A treatment of these systems is more difficult since the observed value of  $M \sin^3 i$  is very uncertain and since opacities for the secondary's cool interior are needed. We also excluded hotter systems with shallow envelopes since they require a more refined treatment of convection in the outermost mass shells than in the present code.

Finally, the discussion concerned only systems in good thermal contact.

Taking into account these restrictions we conclude that many (possibly all) observed contact binaries evolve on a thermal time-scale, probably in thermal cycles as proposed by Lucy (1976) and Flannery (1976). This raises the old problem that the semi-detached phase is apparently not observed among shortest-period systems ( $P \lesssim 0.35$  days). Note that most systems discussed in this paper belong to this class.

We investigated many theoretical equilibrium configurations with realistic combinations of observable properties (period, mass ratio, temperature difference etc.), including configurations violating the contact condition. In all configurations evolutionary effects are important ( $X_c < 0.4$ ). Moreover, in a generalised thermal stability problem all configurations turned out to be unstable on a time scale of  $(3 \dots 7) 10^7$  yr. (In view of the large differences between the observed systems this time interval is remarkably small.) Accordingly, the structure of unevolved real contact binaries is usually incompatible with thermal equilibrium. The structure of evolved real systems is in some cases compatible with thermal equilibrium but usually not with stable equilibrium.

For unrealistic combinations of observable properties, however, stable thermal equilibrium is possible, even in unevolved configurations. For example, Hazlehurst et al. (1982), Hazlehurst & Refsdal (1984) and Kähler et al. (1987) found unevolved stable solutions (Biermann-Thomas models). They are highly unrealistic since the temperature difference is very large. The stability of these models is compatible with the present discussion since the entropy difference is very large and since Eq. (19) with positive values for  $m$  and  $n$  is used. Symmetrical or nearly symmetrical stable systems (Kähler et al. 1987) are also unrealistic since mass ratios close to unity are not observed.

More interesting is a stable evolved configuration with a small entropy difference ( $\Delta S = 0.24$ ) found by Refsdal & Stabell (1981), using Eq. (19) with  $m = 4.5, n = 2$ . The parameters of this configuration are probably unrealistic as indicated by angular momentum problems. Evolutionary effects are larger than in the configurations discussed in the present paper. (Hydrogen in the primary's centre is exhausted.) These effects have a stabilizing influence. This explains the stability.

Equally interesting is a stable evolved configuration found by Robertson & Eggleton (1977). The configuration is in shallow contact and has a small temperature difference and typical values for mass ratio ( $q = 0.42$ ) and period ( $P = 0.40$  days).

These examples show that from a purely theoretical viewpoint the existence of contact systems in thermal equilibrium cannot be excluded if major evolutionary effects are invoked. This paper was concerned with a quite different problem. We asked whether real (observed) contact binaries are in thermal equilibrium. As we have seen, this problem can usually be solved if sufficient observational information is available. All systems investigated so far turned out to be in thermal disequilibrium.

**References**

- Batten A.H., Lu W., 1985, PASP 98, 92  
Flannery B.P., 1976, ApJ 205, 217  
Hazlehurst J., Höppner W., Refsdal S., 1982, A&A 109, 117  
Hazlehurst J., Refsdal S., 1980, A&A 84, 200  
Hazlehurst J., Refsdal S., 1984, A&A 133, 63  
Hrivnak B.J., 1988, ApJ 335, 319  
Hrivnak B.J., 1989, ApJ 340, 458  
Kähler H., 1995, A&A 294, 497  
Kähler H., Matraka B., Weigert A., 1987, A&A 172, 179  
Kaluzny J., Ruciński S.M., 1986, AJ 92, 666  
Kippenhahn R., Weigert A., 1990, Stellar Structure and Evolution, Springer, Berlin  
Lapasset E., Gómez M., 1990, A&A 231, 365  
Linnell A.P., 1991, ApJ 379, 338  
Lu W.-X., 1986, PASP 98, 577  
Lu W.-X., Ruciński S.M., 1993, AJ 106, 361  
Lucy L.B., 1967, Z. Astrophys. 65, 89  
Lucy L.B., 1976, ApJ 205, 208  
Olsen E.H., 1984, A&AS 57, 443  
Philip A.G.D., Relyea L.J., 1979, AJ 84, 1743  
Refsdal S., Stabell R., 1981, A&A 93, 297  
Robertson J.A., Eggleton P.P., 1977, MNRAS 179, 359  
Ruciński S.M., 1983, A&A 127, 84  
Ruciński S.M., Kaluzny J., 1982, Astrophys Space Sci. 88, 433  
Ruciński S.M., Lu W.-X., Shi J., 1993, AJ 106, 1174  
Webbink R.F., 1977, ApJ 215, 851  
Yamasaki A., 1979, Astrophys. Space Sci. 60, 173